ce/papers Proceedings in civil engineering

Ernst & Sohn A Wiley Brand

ORIGINAL ARTICLE

eurosteel AMSTERDAM 2023

Ernst & Sohn A Wiley Brand

Hysteretic behaviour of welded connections with highly inelastic panel zones

Andronikos Skiadopoulos[1] | Dimitrios G. Lignos[1] | Masaki Arita[2] | Satoru Hiroshima[2]

Correspondence

Dr. Andronikos Skiadopoulos
Civil Engineering Institute, ENAC, École Polytechnique Fédérale de Lausanne (EPFL), Station 18, Lausanne 1015, Switzerland
Email: andronikos.skiadopoulos@epfl.ch

[1] École Polytechnique Fédérale de Lausanne (EPFL), Dept. Architecture, Civil and Environmental Engineering, Lausanne, Switzerland
[2] Nippon Steel Corporation, Dept. of Research and Development, Chiyoda, Tokyo, Japan

Abstract

The current practice in capacity-designed steel moment resisting frames (MRFs) worldwide allows for limited shear yielding in the column web panel zone. As such, inelastic deformations concentrate near the beam ends, thereby leading to flexural strength deterioration due to local buckling often at modest lateral drift demands. Experiments on post-Northridge welded connections suggest that prior to a story drift angle of 5% rad, panel zone kinking does not induce fracture for panel zone shear distortions of up to $10\gamma_y$. Within such a context, this paper presents an alternative design of a welded moment connection with highly inelastic panel zones. The connection features simplified weld details including a customised beveled backing bar that can be kept in place after the completion of the complete joint penetration welds at the beam flange-to-column flange joint. Full scale experiments suggest that the hysteretic response of the connection remains stable up until a story drift angle of 8% rad. The specimen did not exhibit visible structural damage prior to story drift angles of 4% rad, which are characteristic to a maximum considered earthquake. Modest local buckling occurred near the beam ends only after a story drift angle of 5% rad, which is a typical drift threshold in current collapse assessment methodologies. This paper summarises the primary findings of the experimental program for one of the test specimens.

Keywords

Steel moment resisting frames, Beam-to-column connections, Welded connections, Backing bars, Inelastic panel zones, Instability-free performance

1 Introduction

The seismic stability of capacity-designed steel moment resisting frames (MRFs) relies on the hysteretic behaviour of their beam-to-column connections. Current seismic standards allow for limited inelastic deformations within the column web panel zone [1]–[4]. In such a design context, steel beams are likely to exhibit inelastic geometric instabilities, i.e., local buckling, throughout earthquake loading.

After the 1994 Northridge earthquake, the design practice focused on connection design with fairly limited panel zone yielding [5]–[8]. Investigations following the 1994 Northridge earthquake demonstrated that connection fractures at lateral drift demands of 1-2% or less were attributable mainly to a combination of factors, such as: (a) the inelastic panel zone behaviour [9], [10], (b) the utilisation of weld metals with low toughness and poor quality control, (c) the weld access hole geometry [11]–[13], and (d) the presence of the weld backing bar at the bottom beam flange-to-column flange joint that created a notch condition at that highly stressed region.

To date, the detailing of prequalified welded unreinforced flange-welded web (WUF-W) connections [14] is depicted in Figure 1a. It is meant to reduce the fracture potential at the beam flange-to-column flange joint. This is achieved by utilising toughness-rated weld metals; by employing an optimised access hole geometry [13]; and by applying a stingent treatment in the bottom beam flange-to-column face welding process. This treatment includes removal of the weld backing bar, back-gouging and fillet weld reinforcement, as shown in Figure 1b. Panel zone yielding is also limited.

Although the bottom beam flange-to-column flange joint weld detailing treatment minimizes the fracture potential at this location, it is a time and recourse consuming process [5], [15], [16]. In recent work, Skiadopoulos and Lignos [17] proposed, via finite element simulation-assisted design, a customised beveled backing bar that can be potentially kept in place after the execution of the complete joint penetration (CJP) welds at the beam flanges (see Figure 1c). The beveled backing bar, which can be kept in place after the CJP weld completion, minimises the fracture potential at the beam flange-to-

https://doi.org/10.1002/cepa.2676 wileyonlinelibrary.com/journal/cepa

column face welded connection.

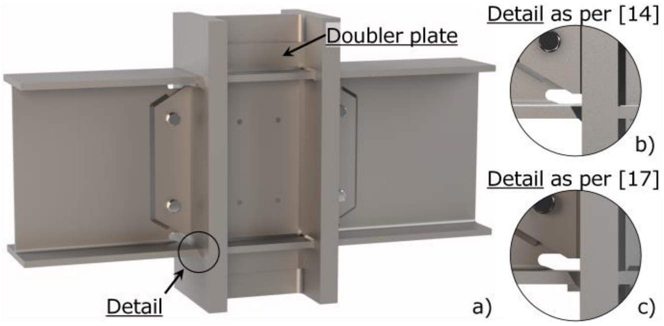

Figure 1 a) Typical welded unreinforced-flange welded web beam-to-column connection, and b-c) beam flange-to-column face welded detail according to AISC [14] and Skiadopoulos and Lignos [17], respectively

Experimental evidence demonstrates that welded moment connections designed according to the current seismic provisions respect the prequalification criteria [18]. Although this is satisfactory from a life-safety standpoint, structural damage in the form of beam end local buckling and strength/stiffness degradation may be evident at modest lateral drift demands, as shown in Figures 2a-b [19]. However, by considering a nominally identical connection without doubler plates, a stable hysteretic response is achieved in the connection up until lateral drift demands exceeding 6% (see Figures 2a and 2c). Some of these observations date back to 1970s [20], [21] and were recently highlighted in experimental work that mobilised inelastic panel zones, exceeding shear distortions of $10\gamma_y$ (where γ_y is the panel zone shear distortion at yield) [19], [22]–[24].

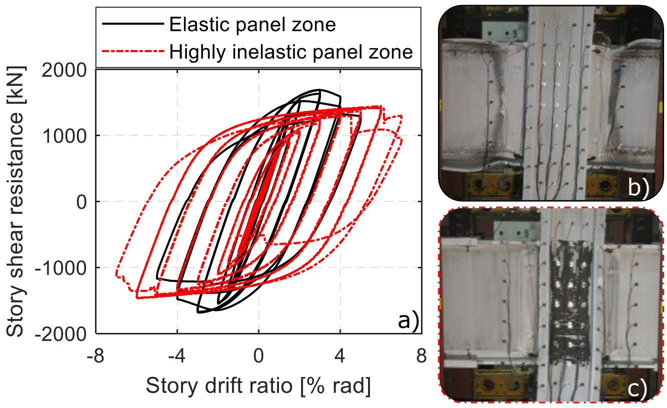

Figure 2 a) Hysteretic response of welded moment connections featuring elastic and highly inelastic panel zones, and b-c) deformed shapes at 4% story drift ratio of the elastic and highly inelastic panel zone design cases, respectively {data and images adopted from [19]}

In steel MRFs, deep columns is a common practice [25], [26]. When panel zone yielding is promoted, the column twisting demands due to beam end instabilities reduce [27], [28]. Limited structural damage in the connection should also be anticipated. Moreover, comprehensive system-level steel MRF studies have demostrated the reduction of residual story drift ratios in the aftermath of earthquakes [29]. Finally, panel zone yielding enables simpler fabrication because of the anticipated reduction of doubler plates within the colum web panel relative to its elastic panel zone counterpart.

Within such a context, this paper introduces a new welded beam-to-column connection typology that defies the currect paradigm in WUF-W connections. The proposed connection employs: (a) simplified weld details by keeping a customised beveled backing bar in place after the execution of the CJP welds between the beam(s) flanges and the column flange(s), (b) highly inelastic panel zones, and (c) minimum through-thickness material toughness requirements for the column flanges. The potential of the proposed connection typology is demonstrated by means of full-scale interior subassembly experiments.

2 Overview of the testing program

2.1 Test objectives

The panel zone resistance (as per Skiadopoulos et al. [30]) over demand ratio, R_n/R_u, is assumed to be equal to 0.8, contrary to 1.0 that is the permissible design limit in the current seismic provisions [1]. As such, the panel zone is anticipated to reach inelastic shear distortions of up to $15\gamma_y$ at lateral drift demands characteristic of a maximum-considered earthquake event (i.e., 3-4%). Nonlinear geometric instabilities in the steel beam ends are prevented prior to the same story drift angle amplitude. As a consequence, structural repairs in connections are not deemed to be necessary after a design-basis earthquake. Moreover, a sufficient reserve capacity is ensured in the connection to sustain the demands during a typical mainshock-aftershock earthquake sequence.

2.2 Test specimen and apparatus

The interior beam-loaded beam-to-column subassembly features an H498x432x45/70 steel column with 70 mm flange thickness and HY650x300x16x25 steel beams with 650 mm depth. In North America, the above cross sections are equivalent to a W14x398 and a W24x131, respectively. The column is made of SM490A and the beams of SN490B, with a nominal yield strength of 325 MPa. The strong column-weak beam ratio in this case is nearly equal to two.

The selected beam depth and the moderate web and flange local slenderness ratios of the beam cross section (i.e., 35.9 and 6, respectively) are likely to cause increased strain demands in the beam flange-to-column flange joints [9].To prevent lamellar tearing and divot fracture in the thick column flanges [15], [31], minimum toughness requirements are imposed in the through-thickness direction of the column material to match those of the demand critical CJP welds.

A welded WUF-W connection is realised, as illustrated in Figure 3. This features: (a) top and bottom beveled backing bars without reinforcing fillet welds [17], (b) no doubler plates due to the R_n/R_u of 0.8, (c) an access hole geometry as per AISC [14], and (d) no continuity plates for the selected column cross section [14].

The construction sequence of the beam-to-column connection was performed with the specimen in the upright position, to simulate realistic field weld conditions. The assembling and fabrication sequence of the test specimen followed standard practice [14], [32]. Preheating of the weld region at 50°C preceded the execution of the CJP.

The demand critical CJP welds of the beam flanges and the web were performed based on the gas metal arc welding (GMAW) process. Ultrasonic testing in the CJP welds did not indicate any discontinuities that exceeded the limits of current weld practice [32].

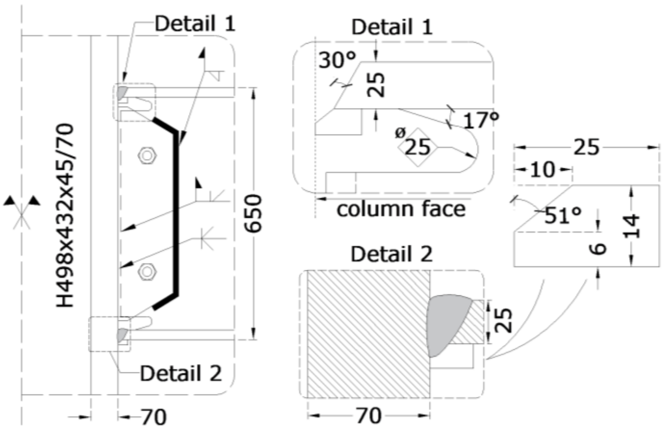

Figure 3 Test specimen beam-to-column connection detail (units: mm)

Referring to Figure 4, the pin-to-pin column distance equals nearly 3400 mm, while the inflection point-to-inflection point beam distance equals 8000 mm. This leads to a beam shear span-to-depth ratio of nearly 6, which is smaller than the allowable limit for special moment frames [14]. Consequently, increased shear demands are expected in the welded connection, which is a conservative assumption in this case.

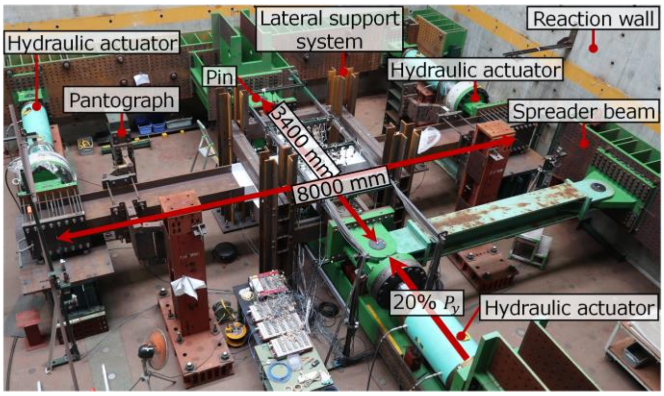

Figure 4 Test setup of the experimental campaign

The beam-loaded test specimen was subjected to the cyclic-symmetric loading protocol of AISC [1] until at least a 80% loss of the connection load-carrying capacity. Two hydraulic actuators operated in displacement control and reacted in a reaction wall through spreader beams (see Figure 4). The test specimen was supported laterally through pantographs and a lateral support system designed as per AISC [1]. The pantographs were positioned near the load application points. A pinned connection was realised at one column end, while at the other one a constant compressive axial load of $0.2P_y$ (where P_y is column axial yield strength) was applied through a roller support.

2.3 Instrumentation and deduced measurements

The test specimen was instrumented with 171 sensors, including uniaxial strain and rosette gauges, linear variable differential transformers (LVDTs) and string potentiometers. The story drift ratio calculation considered a correction due to rigid body motion, through a set of LVDTs positioned at each beam load application and column reaction point. The panel zone shear distortion, γ, was deduced from a set of diagonal LVDTs that were attached to the column flanges at the beam flange level. For redundancy in the measurements, a pair of LVDTs was also mounted to the column web, as shown in Figure 5. The beam and column chord rotations were calculated based on a set of LVDTs positioned perpendicularly and parallel to the column face plane, at the beam flange level (see Figure 5). More details on the deduced measurements of the experimental program are found in Skiadopoulos [33].

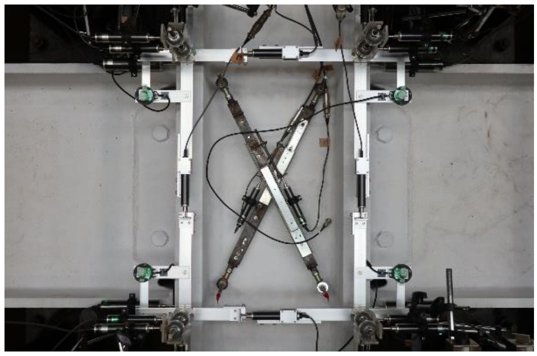

Figure 5 Instrumentation of the beam-to-column connection

3 Experimental results

Figure 6 depicts the story shear resistance versus story drift ratio of the test specimen discussed herein. Superimposed in the same figure are characteristic damage states of interest to the engineering profession. The test specimen remained elastic up until lateral drift demands of 1% where panel zone yielding initiated, as identified by the rosette gauge mounted at the centre.

At lateral drift demands that are characteristic of a design-basis earthquake event (i.e., 2%), both beams yielded at their flanges. The panel zone reached a shear distortion of $4\gamma_y$. At that drift level, there was no observable damage in the beam-to-column connection. Similar observations hold true for a story drift angle of 3%, where the panel zone reached a shear distortion of $8\gamma_y$.

At a lateral drift demand of 4%, the story shear resistance stabilised. The panel zone reached $10\gamma_y$ and the beam did not experience localised deformations, thereby satisfying the anticipated design objectives. At this drift level, there was no indication of damage in the beveled backing bars. At the beam flange-to-column face region, localised yielding was observed due to panel zone kinking.

Upon further loading, beam localised deformations became evident at lateral drift demands of 5-6%. At that drift level, the panel zone reached the targeted design distortion of $15\gamma_y$. The load-carrying capacity of the connection was stable up until 7% (see Figure 6). At 7%, ductile tearing was observed at the column flanges, near the CJP weld toes of both beams' top flanges, near the beam web centreline region. The cracks propagated in a stable manner in the subsequent cycles through the thickness and the longitudinal direction of the column flanges. At 8%, the connection could still withstand more than 90% of $V_{c,max}$ (where $V_{c,max}$ is the peak story shear resistance), while at the first excursion of 9%, the connection lost 20% of its load-carrying capacity. The testing program terminated at the second excursion of 9% drift amplitude.

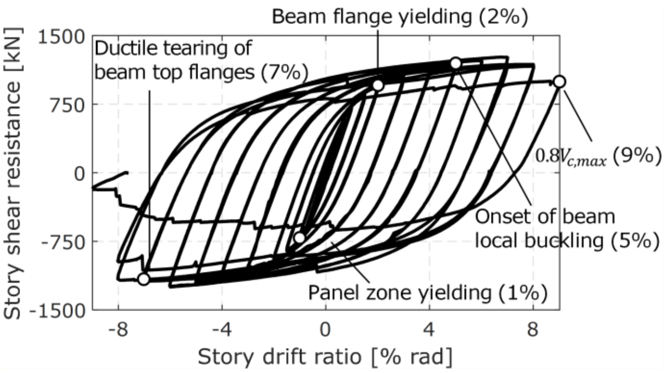

Figure 6 Story shear resistance versus story drift ratio of the test specimen

The welded moment connection demonstrated a stable hysteretic response up until a lateral drift demand of 7%. It should be stated that the AISC [1] symmetric cyclic loading protocol is considered to be very conservative in assessing the response of structural components at lateral drift demands higher than 2% [34]. Therefore, guaranteeing instability-free performance up to a lateral drift demand of 7% is noteworthy stating. The ultimate failure modes involved ultra-low-cycle fatigue initiating at the column flanges near the weld toes of the CJP welds of the beam top flanges, as characteristically shown in Figure 7 for the west beam.

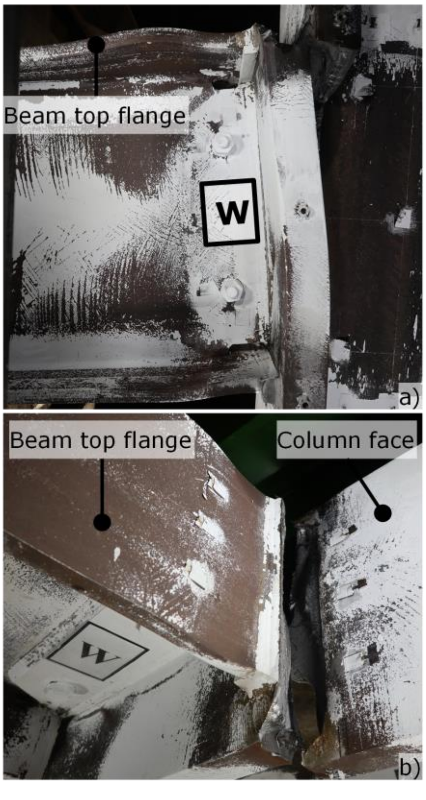

Figure 7 Ultimate failure mode at the west beam after the end of the test

3.1 Balanced inelastic deformations

The experimental results highlighted that the proposed connection withstands more than 80% of its load-carrying capacity up until a story drift angle of 9%. This exceeds the connection prequalification limit of 4% [1]. Figures 8a and 8b depict the local hysteretic responses in terms of panel zone shear force versus normalised shear distortion and east beam end moment versus chord rotation, respectively. The east and west beams had a nearly identical hysteretic response. The local responses are shown up until a lateral drift demand of 7%, where the ductile crack initiation at the column flange near the west beam's top flange CJP weld toe became visually evident. Referring to Figure 8a, the panel zone distortion reached nearly $15\gamma_y$, which corresponds to a 60% contribution to the total story drift ratio of the beam-to-column subassembly. At the same drift demand of 7%, the beam contributed the rest of the plastic deformation to the total story drift ratio.

From Figure 8b, it is evident that the beams exhibited a very stable hysteretic response. The overall connection performance is attributable to the balancing of inelastic deformations between the panel zone and the beams. The instability-free performance of the steel beams suggests no repair actions in the aftermath of a design-basis earthquake. Moreover, the connection can reliably provide appreciable reserve capacity in a mainshock-aftershock earthquake series.

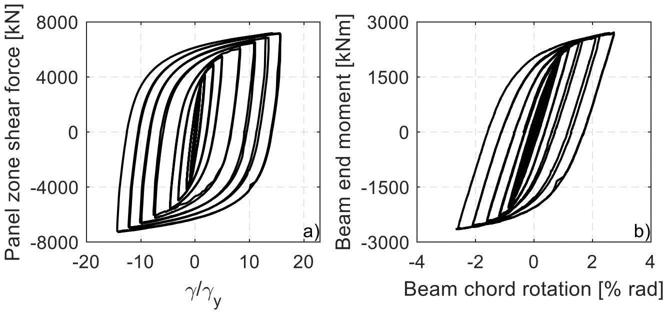

Figure 8 Test specimen experimental results: a) Panel zone force versus normalised distortion response, and b) beam end moment versus chord rotation response

4 Performance of beveled backing bars

Referring to the top beam flange-to-column face welded connection, there was no sign of crack initiation starting from the tip of the backing bar physical notch, even at a story drift angle of 9%. In prior tests on prequalified welded connections, the top beam flange backing bars remained intact as well, and did not experience fracture at the same location [18].

Herein, similar observations hold true for the bottom beam flange backing bars, as characteristically shown in Figure 9a for the west beam bottom beam flange. Figure 9b suggests that near the beam web centreline there was no crack initiating from the tip of the beveled backing bar based on macro-etching observations. As for the east beam bottom flange, ductile crack propagation at the column face was observed at a story drift angle of 8%, near the CJP weld toe.

In brief, the customised beveled backing bar detail is a promising detail that minimises stress concentration at its physical notch because of the stress flow interruption. This has been demonstrated via continuum finite element simulations by prior work of Skiadopoulos and Lignos [17].

Figure 9 a) West beam bottom flange at lateral drift demands of 9% rad, and b) macro-etching observations of the west beam bottom flange backing bar

5 Conclusions

This paper summarizes an experimental program that characterized the hysteretic behaviour of welded unreinforced flange-welded web connections designed with highly inelastic panel zones and simplified weld details through physical experimentation. The interior full-scale subassembly featured: (a) inelastic panel zone design to delay the onset of beam local buckling after a story drift angle of 4%, (b) a customised beveled backing bar that minimises the fracture potential at the beam flange-to-column flange joint [17], and (c) specified minimum toughness requirements in the through-thickness direction of the column material to prevent divot fracture.

The following observations hold true:

At lateral drift demands characteristic of design-basis earthquake events (i.e., 2%), the proposed connection experienced panel zone and beam yielding, without any notable signs of structural damage.

At lateral drift demands representative of maximum-considered earthquake events (i.e., 3-4%) the panel zone attained a shear distortion of about $10\gamma_y$. The beams did not experience local instabilities; hence, the connection did not exhibit strength and/or stiffness degradation under cyclic loading.

Local buckling in the steel beam flanges was visible only after a story drift angle of 5%. However, in-cycle strength and stiffness deterioration did not become evident up until a lateral drift angle of 7-8%.

Ductile crack initiation at the column faces near the complete joint penetration weld toes of the beam top flanges was observed at a story drift angle of 7%. These cracks initiated near the beam web centrelines and propagated in a stable manner in the thickness and longitudinal direction of the column flanges throughout loading. The connection was able to dissipate one third of the total dissipated energy from the onset of crack initiation to the loss of at least 80% of its lateral load-carrying capacity.

There was no observable sign of damage in the beveled backing bars up until a story drift angle of 8%. This is attributed to the optimal bevel design that interrupts the stress flow at the tip of the physical notch of the backing bar. Further details regarding the entire experimental program may be found in [35].

Acknowledgements

The work of this study is based on a collaborative grant with Nippon Steel Corporation, as well as an EPFL internal grant. The financial support is gratefully acknowledged. The authors would also like to sincerely thank Dr. Yusuke Suzuki (Senior Manager at Nippon Steel Corporation) for several insightful discussions, as well as the personnel of the Hasaki laboratory of Nippon Steel Corporation. The authors would also like to thank Techno Steel Daishin for fabricating the test specimens, Mr. Kenta Yoshiba who conducted the welding, and Mr. Shun Ri for performing ultrasonic testing in the welds. Any opinions, findings, and conclusions or recommendations expressed in this paper are those of the authors and do not necessarily reflect the views of sponsors.

References

[1] AISC (2016) *Seismic provisions for structural steel buildings*. Chicago, IL, USA: American Institute of Steel Construction, Report Nr. ANSI/AISC 341-16.

[2] CEN (2005) *EN 1993-1-8: Eurocode 3: Design of steel structures – Part 1-8: Design of joints*. Brussels, Belgium: European Committee for Standardization.

[3] CSA (2019) *Design of steel structures*. Mississauga, Canada: CSA, Report Nr. CAN/CSA S16-19.

[4] AIJ (2012) *Recommendations for design of connections in steel structures*. Architectural Institute of Japan, Tokyo (in Japanese).

[5] FEMA (2000) *State of the art report on connection performance*. Washington, DC, USA: Federal Emergency Management Agency, Report Nr. FEMA-355D.

[6] Malley, J.O. (1998) *SAC steel project: summary of phase 1 testing investigation results*. Engineering Structures 20, H. 4–6, pp. 300–309, https://doi.org/10.1016/S0141-0296(97)00033-3.

[7] Mahin, S.A. (1998) *Lessons from damage to steel buildings during the Northridge earthquake*. Engineering Structures 20, H. 4–6, pp. 261–270, https://doi.org/10.1016/S0141-0296(97)00032-1.

[8] Miller, D.K. (1998) *Lessons learned from the Northridge earthquake*. Engineering Structures 20, H. 4, pp. 249–260, https://doi.org/10.1016/S0141-0296(97)00031-X.

[9] El-Tawil, S.; Vidarsson, E.; Mikesell, T.; Kunnath, S.K. (1999) *Inelastic behavior and design of steel panel zones*. Journal of Structural Engineering 125, H. 2, pp. 183–193, https://doi.org/10.1061/(ASCE)0733-9445(1999)125:2(183).

[10] Chi, W.-M.; Deierlein, G.G.; Ingraffea, A. (2000) *Frac-*

ture toughness demands in welded beam-column moment connections. Journal of Structural Engineering 126, H. 1, pp. 88–97, https://doi.org/10.1061/(ASCE)0733-9445(2000)126:1(88).

[11] Lu, L.W.; Ricles, J.M.; Mao, C.; Fisher, J.W. (2000) *Critical issues in achieving ductile behaviour of welded moment connections*. Journal of Constructional Steel Research 55, H. 1–3, pp. 325–341, https://doi.org/10.1016/S0143-974X(99)00092-9.

[12] Mao, C.; Ricles, J.; Lu, L.W.; Fisher, J. (2001) *Effect of local details on ductility of welded moment connections*. Journal of Structural Engineering 127, H. 9, pp. 1036–1044, https://doi.org/10.1061/(ASCE)0733-9445(2001)127:9(1036).

[13] Ricles, J.M.; Fisher, J.W.; Lu, L.-W.; Kaufmann, E.J. (2002) *Development of improved welded moment connections for earthquake-resistant design*. Journal of Constructional Steel Research 58, H. 5–8, pp. 565–604, https://doi.org/10.1016/S0143-974X(01)00095-5.

[14] AISC (2016) *Prequalified connections for special and intermediate steel moment frames for seismic applications*. Chicago, IL, USA: American Institute of Steel Construction, Report Nr. ANSI/AISC 358-16.

[15] Miller, D.K. (2017) *AISC steel design guide 21 welded connections - a primer for engineers, 2nd edition*. Chicago (IL): American Institute of Steel Construction.

[16] Popov, E.P.; Yang, T.-S.; Chang, S.-P. (1998) *Design of steel MRF connections before and after 1994 Northridge earthquake*. Engineering Structures 20, H. 12, pp. 1030–1038, https://doi.org/10.1016/S0141-0296(97)00200-9.

[17] Skiadopoulos, A.; Lignos, D.G. (2022) *Proposed backing bar detail in welded beam-to-column connections for seismic applications*. Journal of Structural Engineering 148, H. 8, p. 04022102, https://doi.org/10.1061/(ASCE)ST.1943-541X.0003374.

[18] Skiadopoulos, A.; Lignos, D.G. (2021) *Development of inelastic panel zone database*. Journal of Structural Engineering 147, H. 4, p. 04721001, https://doi.org/10.1061/(ASCE)ST.1943-541X.0002957.

[19] Shin, S. (2017) *Experimental and analytical investigation of panel zone behavior in steel moment frames*. PhD Thesis, Department of Civil, Architectural and Environmental Engineering, University of Texas at Austin, TX, USA.

[20] Krawinkler, H.; Bertero, V.V.; Popov, E.P. (1971) *Inelastic behavior of steel beam-to-column subassemblages*. University of California, Berkeley, CA, USA, Report Nr. 71/07.

[21] Popov, E.P.; Amin, N.R.; Louie, J.J.C.; Stephen, R.M. (1985) *Cyclic behavior of large beam-column assemblies*. Earthquake Spectra 1, H. 2, pp. 203–238, https://doi.org/10.1193/1.1585263.

[22] Lin, K.C.; Tsai, K.C.; Kong, S.L.; Hsieh, S.H. (2000) *Effects of panel zone deformations on cyclic performance of welded moment connections*. in *Proc., 12th World Conference on Earthquake Engineering (WCEE)*, New Zealand National Society for Earthquake Engineering, Auckland, New Zealand.

[23] Rahiminia, F.; Namba, H. (2013) *Joint panel in steel moment connections, part 1: experimental tests results*. Journal of Constructional Steel Research 89, pp. 272–283, https://doi.org/10.1016/j.jcsr.2013.07.002.

[24] Kim, S.-Y.; Lee, C.-H. (2017) *Seismic retrofit of welded steel moment connections with highly composite floor slabs*. Journal of Constructional Steel Research 139, pp. 62–68, https://doi.org/10.1016/j.jcsr.2017.09.010.

[25] Elkady, A.; Lignos, D.G. (2018) *Full-scale testing of deep wide-flange steel columns under multiaxis cyclic loading: loading sequence, boundary effects, and lateral stability bracing force demands*. Journal of Structural Engineering 144, H. 2, p. 04017189, https://doi.org/10.1061/(ASCE)ST.1943-541X.0001937.

[26] Ozkula, G.; Harris, J.; Uang, C.-M. (2017) *Observations from cyclic tests on deep, wide-flange beam-columns*. Engineering Journal 54, H. 1, pp. 45–60.

[27] Zhang, X.; Ricles, J.M. (2006) *Experimental evaluation of reduced beam section connections to deep columns*. Journal of Structural Engineering 132, H. 3, pp. 346–357, https://doi.org/10.1061/(ASCE)0733-9445(2006)132:3(346).

[28] Chi, B.; Uang, C.-M. (2002) *Cyclic response and design recommendations of reduced beam section moment connections with deep columns*. Journal of Structural Engineering 128, H. 4, pp. 464–473, https://doi.org/10.1061/(ASCE)0733-9445(2002)128:4(464).

[29] Skiadopoulos, A.; Lignos, D.G. (2022) *Seismic demands of steel moment resisting frames with inelastic beam-to-column web panel zones*. Earthquake Engineering & Structural Dynamics 51, H. 7, pp. 1591–1609, https://doi.org/10.1002/eqe.3629.

[30] Skiadopoulos, A.; Elkady, A.; Lignos, D.G. (2021) *Proposed panel zone model for seismic design of steel moment-resisting frames*. Journal of Structural Engineering 147, H. 4, p. 04021006, https://doi.org/10.1061/(ASCE)ST.1943-541X.0002935.

[31] CEN (2005) *EN 1993-1-10: Eurocode 3: Design of steel structures - Part 1-10: Material toughness and through-thickness properties*. Brussels, Belgium: European Committee for Standardization.

[32] AWS (2016) *Structural welding code-seismic supplement*. American Welding Society, Miami, FL, USA., Report Nr. AWS D1.8/D1.8M:2016.

[33] Skiadopoulos, A. (2022) *Welded moment connections with highly dissipative panel zones for enhanced seismic performance of steel moment frames*. PhD Thesis, École polytechnique fédérale de Lausanne. https://doi.org/10.5075/epfl-thesis-9513.

[34] Krawinkler, H. (2009) *Loading histories for cyclic tests in support of performance assessment of structural components*. in *Proc., 3rd Int. Conf. on Advances in Experimental Structural Engineering*, Pacific Earthquake Engineering Research Center, San Francisco, CA, USA.

[35] Skiadopoulos, A.; Lignos, D.G.; Arita, M.; Hiroshima, S. (2023) *Full-scale experiments of cyclically loaded welded moment connections with highly dissipative panel zones and simplified weld details (accepted)*. Journal of Structural Engineering, https://doi.org/10.1061/JSENDH/STENG-12128.